

Scattering of atoms by the forces of stimulated radiation pressure

V. A. Grinchuk, A. P. Kazantsev, E. F. Kuzin, M. L. Nagaeva,
G. A. Ryabenko, G. I. Surdutovich, and V. P. Yakovlev

P. N. Lebedev Institute of Physics, Academy of Sciences of the USSR, Moscow
(Submitted 17 June 1983)

Zh. Eksp. Teor. Fiz. **86**, 100–109 (January 1984)

A theoretical and experimental study is presented of the effect of stimulated radiation pressure (SRP) under the conditions of strong saturation of the resonance transition when the interaction times between the atom and the field are short (shorter than the radiative lifetime). An experimental method for studying the scattering of an atomic beam by the field of a standing light wave is described. The measured dependence of the scattering efficiency on the electric field and the detuning from resonance is reported. Experimental relationships are compared with theoretical calculations based on the quasiclassical description of the motion of atoms in the field of a light wave, using the effective potential. It is shown that the efficiency of scattering of atoms by SRP forces is of the order of unity in relatively weak (100–1000 V/cm) laser fields. The dispersion curve measured at the center of the unperturbed beam in sufficiently strong fields has an uncustomary width that is much greater than the field broadening.

1. INTRODUCTION

The effect of resonance-frequency light on the translational motion of atoms and molecules, due to radiation pressure forces, is an interesting topic in laser physics.^{1–3} Radiation pressure depends on the closeness of the frequency to the resonance value, and on the intensity and spatial structure of the field. In the final analysis, it is determined by the rate of scattering of photons of the incident beam of radiation. In a sufficiently strong inhomogeneous field (such as a standing wave), the situation is dominated by the gradient force due to stimulated emission and absorption of photons.

The simplest way of studying these forces experimentally is to investigate the scattering of atoms by a standing wave field.⁴ This is analogous to the well-known Kapitza-Dirac effect,⁵ in which electrons are diffracted by the grating produced by the field of a standing light wave. The particular feature of resonance-particle scattering is the considerable strength of the effective potential of the atom in the light field. This facilitates the observation of the effect because the stringent requirements imposed by the Bragg condition on the angle of emission is then removed.

A strong gradient force will scatter atoms through appreciable angles when the time of interaction with the field is as short as $\tau \sim 10^{-7}$ – 10^{-8} s. This time can be both longer and shorter than the spontaneous transition time $1/\gamma$. When $\gamma\tau < 1$, the interaction between the atoms and the field is coherent in character, and the scattering process is wholly determined by the gradient force. When $\gamma\tau > 1$, the coherence of the interaction is, in general, violated and fluctuations in the gradient force must be taken into account.

In the experiment performed in Ref. 6, in which an atomic beam was scattered by a stationary standing wave, the transit time was $\tau \sim 10^{-7}$ s and $\gamma\tau \sim 10$. In our own experiments,⁷ we examined the scattering of atoms by a short light pulse of length $\tau \sim 10^{-8}$ s, so that the parameter $\gamma\tau$ was less than unity.¹⁾

We have carried out a detailed study of the stimulated radiation pressure (SRP) effect by examining the scattering

of a sodium atomic beam by a laser standing-wave pulse.

The scattering process is described theoretically in Sec. 2. Sections 3 and 4 report measurements of the angular distribution and its dependence on the field and atomic-beam parameters.

2. THEORY

When light field is strong and $\gamma\tau < 1$, the force acting on a resonance atom is determined by stimulated transitions, and spontaneous transitions can be neglected. The motion of an atom in the field can then be described with the aid of the effective potential.

In a standing-wave field

$$E(x) \exp[-i(\Delta + \omega_0)t], \quad E(x) = E_0 \cos kx,$$

with small detuning Δ from the atomic-transition frequency ω_0 , there will, in general, be two potentials $\pm U(x)$ for a two-level atom, where

$$U(x) = \frac{1}{2} \hbar \Delta [1 + (2dE/\hbar\Delta)^2]^{1/2}, \quad (1)$$

and d is the transition dipole moment.

They constitute the Stark level shifts in the inhomogeneous external field. When the interaction is turned on adiabatically, the atom moves in the potential that corresponds to the ground state as $E_0 \rightarrow 0$. For positive detuning ($\Delta > 0$), this is the potential $U(x)$.

In classical language, the scattering problem can be formulated as follows. The atomic beam propagates along the y axis, and the atoms have zero initial velocity in the direction of the field gradient (x axis). The initial position x_0 of an atom is a random variable that is uniformly distributed within the field period $2\pi/k$. The laser pulse of length τ is defined by the amplitude $E_0(t)$.

To determine the transverse-velocity distribution function for the particles after the interaction has taken place, we must solve the equation of motion

$$m dv/dt = -\partial U/\partial x$$

and average over the initial position:

$$w(v) = \frac{k}{\pi} \int_0^{\pi/\hbar} dx_0 \delta[v - v(x_0, \tau)].$$

In the potential wells $U(x)$, the particle has the characteristic oscillation frequency

$$\Omega = k(U_M/m)^{1/2},$$

that is determined by the potential modulation depth U_M . The scattering process is essentially determined by the parameter $\Omega\tau$. When $\Omega\tau \ll 1$, the field behaves as a short perturbation. The particle undergoes small displacement in the direction of the field gradient, and the transverse velocity communicated to it is given by

$$mv = -\tau \left. \frac{\partial U}{\partial x} \right|_{x=x_0}$$

which is proportional to the interaction time.

In this case, the scattered-particle velocity distribution has the characteristic square-root form⁸

$$w(v) = \frac{1}{\pi} \frac{1}{(v_0^2 - v^2)^{1/2}}, \quad |v| < v_0, \quad (2)$$

$$v_0 = \frac{\tau |\Delta| \hbar k}{2m} \{ [1 + (2dE_0/\hbar\Delta)^2]^{1/2} - 1 \},$$

where v_0 is the maximum velocity that a particle can acquire during its motion in the field $U(x)$. These relationships remain valid to within an order of magnitude for $\Omega\tau \ll 1$. When the time of interaction with the field is increased so that $\Omega\tau > 1$, the scattering process becomes saturated, and the maximum velocity becomes $v_{\max} \sim (dE_0/m)^{1/2}$. The classical theory of atomic scattering for $\gamma\tau < 1$ was examined in Refs. 4 and 9, and the quantum theory in Refs. 8 and 10.

3. EXPERIMENTAL METHOD

The SRP effect can be investigated experimentally as follows. A sodium atomic beam is exposed to a standing-wave pulse at right-angles to the direction of the atomic beam. The SRP force acts in this direction, so that atoms that have entered the region in which the interaction with the field takes place are scattered. The result of exposure to the radiation is that a portion of the atomic beam is broadened.

Figure 1 illustrates the principle of the experiment. A ribbon beam of sodium atoms (the beam size in the region of interaction with the field was 0.2×11 mm) with a divergence

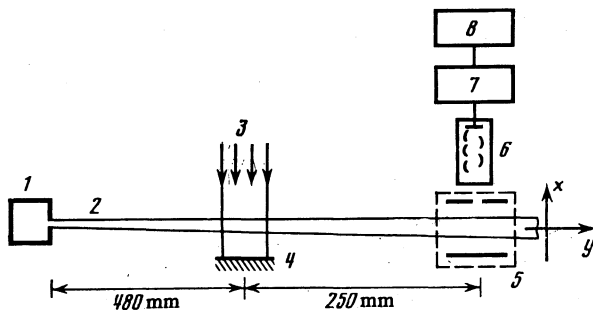


FIG. 1. Schematic illustration of the experimental setup: 1—crucible, 2—atomic beam, 3—laser beam, 4—100% mirror, 5—detector, 6—electron multiplier, 7—amplifier, 8—oscilloscope.

of 5×10^{-4} rad is formed by two 100- μ m slits at a distance of 40 cm from one another. The beam density in the interaction region at the maximum of the distribution is about 3×10^8 cm^{-3} .

The resonance-frequency radiation was produced by a rhodamine-C tunable dye laser, generating pulses with $\tau \sim 10^{-8}$ s. The laser frequency could be tuned in the neighborhood of the $3s_{1/2} \rightarrow 3P_{3/2}$ transition frequency in the sodium atom. The laser linewidth was 0.03 Å, so that the two hyperfine-structure components of the ground state were in resonance. The laser line structure and the detuning from resonance were monitored in the course of these measurements. The parameter $\gamma\tau$ was less than unity.

The standing-wave field was produced with the aid of a mirror placed at a distance of 7 mm from the plane of the ribbon atomic beam. The size of the coherence region in which the standing-wave pattern was established was examined in a special experiment.¹¹ For the laser linewidth of 0.03–0.05 Å, the size of this region was much greater than the distance between the mirror and the atomic beam.

The sodium atoms were detected by exploiting the phenomenon of surface ionization of neutral sodium atoms by a hot tungsten-rhenium wire whose work function was greater than the ionization potential of sodium. The wire was located in the plane of the ribbon beam and could be displaced across the beam by a special micrometer device. The sodium ions produced on the wire surface were accelerated in the space between two plane electrodes, and were finally intercepted by an electron multiplier. Figure 2 shows the distribution of the atoms over the cross section of a stationary, undisturbed beam.

Atoms entering the standing-wave field acquire transverse velocity components. Since the light pulse is short, the displacement of the atoms during the interaction time τ can be neglected. The result is that atoms in the region of intersection of the atomic beam and the light beam are irradiated. The atoms thus acquire transverse velocity components, so that the beam intercepted by the detector becomes broadened. It is also stretched in the axial direction because of the Maxwellian longitudinal-velocity distribution.

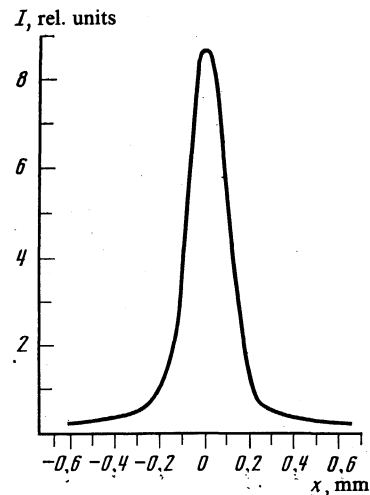


FIG. 2. Beam profile.

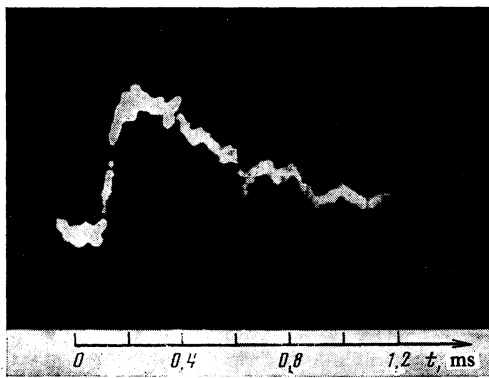


FIG. 3. Typical pulse of scattered atoms recorded by the detector in a given transverse position.

The detector records the particle flux at a given point in space as a function of time. Figure 3 shows a typical current pulse due to scattered atoms. The characteristic time scale of the signal recorded by the detector is determined by the transit time (delay time) between the point of irradiation and the detector. It is given by $t_0 = l/u = 5 \times 10^{-4}$ s, where u is the most probable longitudinal velocity in the beam. It is clear from the figure that, as expected for the Maxwellian velocity distribution, the variance of the delay time is of the order of t_0 . The time t_0 is much longer than the laser pulse length. The "stretching" of the irradiated volume in the longitudinal direction occurs from a value determined by the diameter of the light beam (1–4 cm) to a value equal to the distance to the detector ($l \approx 25$ cm). For each delay time, the detector records a group of atoms with a particular longitudinal velocity. This means that results obtained in this way correspond to measurements with a monoenergetic atomic beam.

Simple calculations yield the following expression for the current pulse due to scattered particles as function of position and time:

$$j(x, t) = \frac{4}{\sqrt{\pi}} \frac{S}{h\lambda} \left(\frac{t_0}{t}\right)^3 \exp\left\{-\left(\frac{t_0}{t}\right)^2\right\} \varphi(x, t), \quad (3)$$

$$\varphi(x, t) = \int dv W(v) f(x-vt) - f(x),$$

where S and h are, respectively, the illuminated area and the height of the atomic beam. The function $f(x)$ describes the shape of the stationary beam (Fig. 2) and is normalized so that $f(0) = 1$; $W(v)$ is the transverse-velocity distribution of the atoms after they have experienced the laser pulse. The latter function is obtained by averaging (2), which corresponds to a particular field intensity, over the intensity distribution across the light beam. The parameter S/h is related to the above stretching of the irradiated volume, and its effective value in our experiments was found to range from 0.04 to 0.16, depending on the light beam diameter. The time dependence of the scattered-particle pulse is largely determined by the Maxwellian factor $(t_0/t)^3$ and is in good agreement with the experimental result shown in Fig. 3. The fact that the particle flux is conserved is described by the expression

$$\int j(x, t) dx = 0.$$

A natural scale, equal to the thickness a of the atomic beam in the region of the detector, arises when the scattering pattern is described in terms of the transverse displacements x . The scattering efficiency depends on the dimensionless parameter

$$\xi(E, \Delta) = v_0 t_0 / a,$$

where v_0 is given by (2). When $\xi \ll 1$, the atomic beam is left by a small fraction of atoms, and the spatial structure of the current pulse has the form

$$\varphi(x, t_0) \approx \frac{1}{2} f''(x) t_0^2 \bar{v}^2 \sim \xi^2 a^2 f''(x), \quad (4)$$

where it is assumed that $W(v)$ is a symmetric function since, otherwise, the first derivative of f would appear.

In a strong field, in which $\xi \gg 1$, most of the particles leave the atomic beam and are displaced to distances that are large in comparison with a . The function φ is then given by

$$\varphi(x, t_0) \approx -f(x), \quad |x| < a, \quad (5)$$

$$\varphi(x, t_0) \approx (v_0/\xi) W(x/t_0), \quad a \ll |x| < a\xi.$$

It is clear that, in the interior of the beam ($|x| < a$), the shape of the signal is essentially the same as the shape of the stationary current pulse, and has the opposite sign. Outside the beam, the shape of the current pulse is determined by the velocity distribution function $W(v)$. The shape of this function depends on the spatial distribution of the field intensity. In particular, for a constant intensity, W is given by (2), and this ensures that $\varphi(x)$ follows the square-root variation as $x \rightarrow a\xi$. The maximum is reached at $x = a\xi$, and its height is of the order of $\sqrt{\xi}$. For other field distributions (for example, the Gaussian distribution), the function $W(x/t_0)$ becomes a monotonically decreasing function for $x > 1.5a - 2a$.

4. EXPERIMENTAL RESULTS

The above experimental arrangement was used to observe the scattering of the sodium atoms⁷ and to determine its dependence on the field parameters. The effect was absent when the mirror producing the standing wave was covered. This confirms that the atoms were, in fact, scattered by SRP forces, since gradient forces are absent in the case of a progressive wave.

Figure 4 shows the amplitude of the detector current due to scattered particles as a function of transverse position. Each point on this graph corresponds to the maximum of the pulsed current as a function of time, i.e., it is determined by the group of beam atoms with longitudinal thermal velocity of 5×10^4 cm/s. Scattered atoms leave the central part of the beam, so that the signal is negative at the center and positive at the edges of the beam and outside the beam.

The laser generated several (1–3) longitudinal modes with an overall width of about 0.03 Å. The center of the mode packet was tuned to the center of the atomic line. The field distribution over the cross section of the laser beam was Gaussian in shape, with $E_0 \sim 3$ kV/cm at maximum. This field (with an effective detuning of about 0.03 Å) corresponds to the displacement of the sodium atoms to a distance of

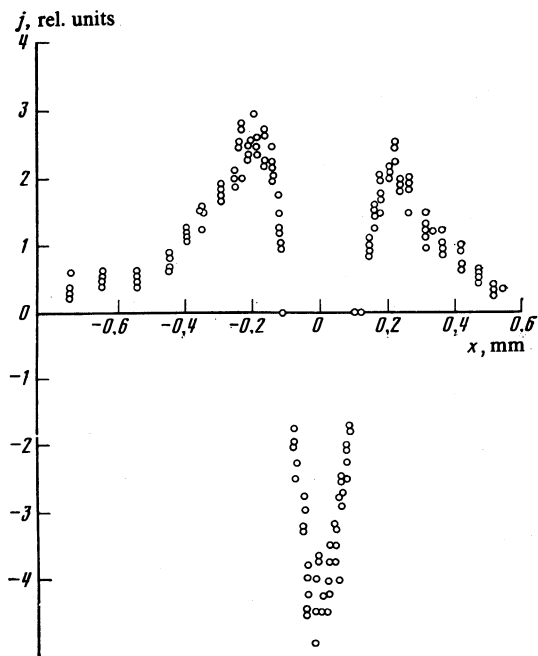


FIG. 4. Alternating component of the detector current due to scattered particles as a function of the transverse position of the detector.

about 5 mm, which is much greater than the width of the atomic beam (~ 0.2 mm), so that $\xi \gg 1$. These atoms determine the distant wings of the angular distribution which, in our experiment, were not observed because of the low signal-to-noise ratio. The positive part of the signal shown in the figure was largely due to particles scattered by the weak field ($\lesssim 500$ V/cm) on the periphery of the laser beam. The shape of the experimental curves describing the angular distribution of scattered particles is in qualitative agreement with the distribution $\varphi(x)$ for the strong field case (5).

The efficiency of scattering can be judged from the size of the negative signal at the beam center. Figure 5 shows the absolute signal strength at the center of the beam as a function of the field strength for a Gaussian (curve 1) and parabolic (curve 2) intensity distribution across the light beam. The field strengths correspond to the distribution maximum. The radiation frequency was tuned to the line center.

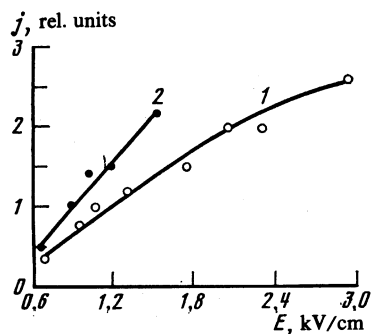


FIG. 5. Signal due to scattered atoms at the center of the beam as a function of the field strength for a Gaussian (1) and a parabolic (2) distribution of laser-beam intensity as a function of position at right-angles to the light beam.

The lower signal strength corresponding to curve 1 was due to the lower effective volume of the interaction region, and the slower variation was connected with the fact that a substantial fraction of the illuminated particles was located in the weak-field region on the periphery of the light beam. These experimental data are in good agreement with calculations of the current at the beam center, based on (3).

We note that the quantity $\varphi(x=0)$ is a measure of the fraction of particles scattered out of the beam. In a very strong field, we see from (5) that $\varphi(0) = -1$, which corresponds to the complete departure of particles from the beam center. For finite fields, $|\varphi(0)| < 1$ and depends not only on the field strength but also on its spatial distribution. Thus, for the Gaussian intensity distribution

$$I/I_0 = \exp(-r^2/r_0^2)$$

the dependence of the signal on the amplitude E of the field strength is

$$|\varphi(0)| \approx \frac{r_a}{R} = \frac{r_0}{R} \left(2 \ln \frac{E}{E_a} \right)^{1/2}, \quad E \gg E_a, \quad (6)$$

where $R = 2$ cm is the mirror radius, $r_0 \approx 0.8$ cm, and $E_a \approx 300$ V/cm for a detuning of the order of the linewidth. The quantity $|\varphi(0)|$ is determined by the effective size of the interaction region, i.e., the radial distance r_a at which the field strength is E_a . The field E_a corresponds to $\xi = 1$, i.e., particle displacement to a distance of the order of the width of the atomic beam. It is clear that (6) is a relatively "slow" logarithmic function. For the parabolic intensity distribution $I/I_0 = 1 - r^2/R^2$, the dependence of the current on the field strength becomes steeper (Fig. 5). For comparison, we also show the graph corresponding to the uniform field (curve 1, Fig. 6), which is given by

$$|\varphi(0)| = \frac{2\xi}{\pi}, \quad \xi < 1,$$

$$|\varphi(0)| = 1 - \frac{2}{\pi} \left[\arcsin \frac{1}{\xi} - \xi + (\xi^2 - 1)^{1/2} \right] \approx 1 - \frac{1}{\pi\xi}, \quad \xi > 1. \quad (7)$$

For simplicity, the shape of the stationary current $f(x)$ was taken in the form of a triangle of width a at half-height.²⁾ It is clear from Fig. 6 that the scattering efficiency increases as

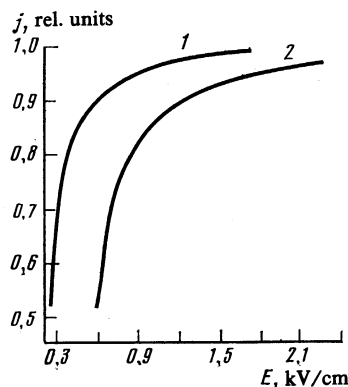


FIG. 6. Theoretical dependence of the signal at the center of the beam on the field strength in the case of a uniform (rectangular) (1) and parabolic (2) intensity distribution; $\delta\lambda_l = 0.03$ Å.

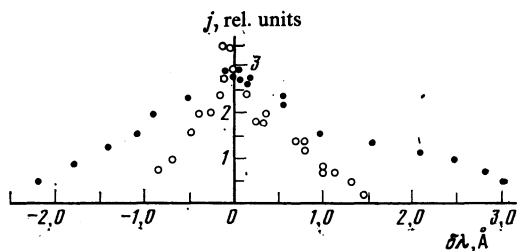


FIG. 7. Signal at the center of the atomic beam as a function of detuning from resonance for two distributions of the laser radiation: ○—parabolic, ●—Gaussian.

the field distribution becomes more homogeneous.

It follows from the experimental data that $|\varphi(0)| \sim 1$ for fields $E > E_a$, i.e., the fraction of scattered particles is of the order of unity. This is also in agreement with the behavior of the angular distribution (Fig. 4), which has a minimum at the beam center.

The frequency dependence of the scattering efficiency is of fundamental interest. Figure 7 shows the signal at the beam center as a function of the detuning from resonance for two laser-field distributions. For the Gaussian distribution, the field strength at the maximum is $E_1 = 3.3$ kV/cm, whereas for the parabolic distribution $E_2 = 1.6$ kV/cm. The field broadening $2dE/\hbar$ is $\delta\lambda_1 = 0.21$ Å in the first case and $\delta\lambda_2 = 0.1$ Å in the second, which is several times greater than the laser linewidth. The frequency was tuned from the linewidth 0.03 to 3 Å.

It is clear from Fig. 7 that the half-widths of the experimental curves are much greater than the field broadening. This is in agreement with theoretical estimates based on (3) and (7). The variation in the signal at the beam center occurs for the $\xi(E, \Delta) \sim 1$. The width of the resonance Δ_0 is then found from the condition $\xi(E, \Delta_0) = 1$. In a strong field, we have

$$\Delta_0 = \frac{dE}{\hbar} \frac{E}{E_a(\Delta=0)}, \quad E_a(\Delta=0) = \frac{ma}{dk\tau v_0} \approx 85 \text{ V/cm}. \quad (8)$$

Thus, under our conditions, the width of the resonance curve exceeds the field broadening $2dE/\hbar$ by a factor of 10–20. This dependence of the resonance width on the field is connected with the particular variation in the signal at the

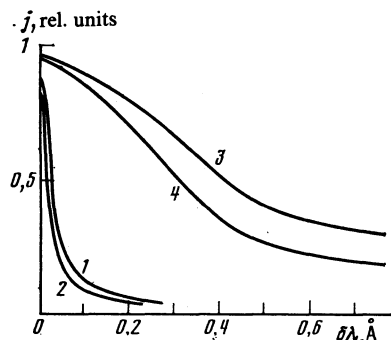


FIG. 8. Theoretical dependence of the signal at the center of the beam on the detuning from resonance for a uniform (rectangular) (1,3) and parabolic (2,4) distribution of intensity and two values of field amplitude: 1, 2— $E_0 = 235$ V/cm, 3, 4—940 V/cm.

center of the beam for high field strengths. In fact, a change in the detuning by $2dE/\hbar$ leads to a change in the wing of the scattered pattern, but the current at the center remains practically constant. It is only for large detuning $\Delta \sim \Delta_0$ that the current at the center of the beam begins to vary appreciably.

In weak fields $E \lesssim E_a$, the width of the resonance is equal to the field broadening.

As an illustration, Fig. 8 shows the calculated wavelength dependence of $|\varphi(0)|$ for rectangular and parabolic intensity distributions and two values of the field amplitude. It is clear from Fig. 8 that, for fields $E \lesssim 200$ V/cm, the width of the dispersion curve is of the order of the field broadening ($\delta\lambda \sim 0.01$ Å) when the scattering efficiency is of the order of unity.

5. CONCLUSIONS

Analysis of experimental data has shown that the scattering efficiency for resonant atoms scattered by a standing light-wave pulse is of the order of unity in relatively weak fields (100–1000 V/cm) produced by a tunable laser beam. The scattered-particle current was measured as a function of frequency for sufficiently strong fields at the center of the atomic beam, where it has the unusual width given by (8). This width depends not only on the field but also on the transverse size of the atomic beam. In our experiments, it was greater by an order of magnitude than the field broadening. The wavelength dependence in the wings of the scattered pattern has the usual field width. However, we have not been able to measure it because of the low signal-to-noise ratio. Estimates show that it is possible to produce a narrow wavelength dependence (with a width of the order of 0.01 Å) for a scattering efficiency of the order of unity if the field is of the order of 200 V/cm and the laser linewidth is reduced by several times.

The experimental results are in agreement with theoretical predictions based on the effective potential for the resonance atom in the standing-wave field.

A particular feature of the motion of an atom in an inhomogeneous light field is the presence of the two potentials $\pm U(x)$ and, correspondingly, two trajectories of motion. In our experiments, the atoms were displaced through distances much smaller than the wavelength during the presence of the laser pulse ($\Omega\tau \ll 1$), and were able to “feel” only the local field value (or, more precisely, its derivative $\partial U/\partial x$). The atoms do not transfer from one trajectory to another (with the exception of a small group of atoms whose initial coordinates lie in the immediate neighborhood of the field nodes). As a result, the characteristic transverse velocity v_0 given by (2) is a smooth function of the detuning from resonance, and has no singularities at small Δ .

When the particles succeed in traversing distances of the order of the wavelength ($\Omega\tau \gtrsim 1$), singularities appear on the dispersion function $v_0(\Delta)$ at $\tilde{\Delta} = (\Omega dE/\hbar)^{1/2}$. They are connected with the transition of atoms from one trajectory to another after passage through the standing-wave nodes (these are the Landau-Zener transitions^{3,9}). The result is that the scattering process assumes the bipotential character.^{12,13} When the atomic beam is incident normally, the bipotential

scattering effects can, in principle, be observed by increasing the pulse length. Another interesting possibility is to use an atomic beam incident obliquely onto a standing wave. The Landau-Zener transitions then produce an asymmetric scattering pattern, and the asymmetry depends on the sign of the detuning.^{12,13} For pulses with $\tau \sim 10^{-8}$ s, these effects can be observed when thermal-velocity atoms enter the field region at an angle $\approx 3^\circ$ to the normal. For fields of 10^4 V/cm, the characteristic detuning from resonance $\tilde{\Delta}$ for which the Landau-Zener transitions take place is 0.01 \AA . This figure is smaller by a factor of about 30 than the field broadening. Thus, the wavelength dependence of the scattering pattern has two characteristic frequencies: a narrow asymmetric resonance with the Landau-Zener frequency is present against the background of the broad resonance with the field frequency.

¹¹In a recently published experimental paper by Moskowitz *et al.* [Phys. Rev. Lett. **51**, 370 (1983)], the condition $\gamma\tau < 1$ was also maintained. In contrast to the present work, however, the measurements were performed in weak fields. Small-angle scattering corresponding to the absorption of several photons was studied.

²In contrast to (4), the linear dependence in (7) for small ξ is connected with the fact that the chosen function $f(x)$ is nonanalytic at $x = 0$.

¹G. A. Askar'yan, Zh. Eksp. Teor. Fiz. **42**, 1567 (1962) [Sov. Phys. JETP **15**, 1088 (1962)].

²A. Ashkin, Phys. Rev. Lett. **24**, 156 (1970); **25**, 1321.

³A. P. Kazantsev, Zh. Eksp. Teor. Fiz. **66**, 1599 (1974) [Sov. Phys. JETP **39**, 784 (1974)]; **67**, 1660 (1974) [40, 825 (1975)].

⁴A. P. Kazantsev and G. I. Surdutovich, Pis'ma Zh. Eksp. Teor. Fiz. **21**, 346 (1975) [JETP Lett. **21**, 158 (1975)]. G. A. Delone, V. A. Grinchuk, A. P. Kazantsev, and G. I. Surdutovich, Opt. Commun. **25**, 399 (1978).

⁵P. L. Kapitza and P. A. M. Dirac, Proc. Chamber. Phil. Soc. **29**, 297 (1933).

⁶A. Arimondo, H. Lew, and T. Oka, Phys. Rev. Lett. **43**, 753 (1979).

⁷V. A. Grinchuk, A. P. Kazantsev, E. F. Kuzin, *et al.*, Pis'ma Zh. Eksp. Teor. Fiz. **34**, 395 (1981) [JETP Lett. **34**, 375 (1981)]; Phys. Lett. A **81**, 136 (1981).

⁸A. P. Kazantsev, G. I. Surdutovich, and V. P. Yakovlev, Pis'ma Zh. Eksp. Teor. Fiz. **31**, 542 (1980) [JETP Lett. **31**, 509 (1980)].

⁹G. A. Delone, V. A. Grinchuk, S. D. Kuzmichev, *et al.*, Opt. Commun. **33**, 149 (1980).

¹⁰R. J. Cook and A. F. Bernhardt, Phys. Rev. A **18**, 2533 (1978).

¹¹V. A. Grinchuk, E. F. Kuzin, S. D. Kuz'michev, M. L. Nagaeva, and G. A. Ryabenko, Prib. Tekh. Eksp. No. 3, 223 (1982).

¹²A. P. Kazantsev, G. I. Surdutovich, and V. P. Yakovlev, Opt. Commun. **43**, 180 (1982).

¹³D. O. Chudesnikov and V. P. Yakovlev, in Vzaimodeistvie lazernogo izlucheniya s rezonansnymi sredami (Interaction of Laser Radiation With Resonance Media), Energoizdat, Moscow, 1982, p. 102.

Translated by S. Chomet